Tomography studies of biological cells on polymer scaffolds

2004 J. Phys.: Condens. Matter 16 S3499

(http://iopscience.iop.org/0953-8984/16/33/011)

INSTITUTE OF PHYSICS PUBLISHING JOURNAL OF PHYSICS: CONDENSED MATTER

J. Phys.: Condens. Matter **16** (2004) S3499–S3510 PII: S0953-8984(04)80221-2

Tomography studies of biological cells on polymer scaffolds

P Thurner[1,2], B Müller[3], U Sennhauser[1], J Hubbell[2] and R Müller[2]

[1] Swiss Federal Laboratories for Materials Testing and Research, Überlandstrasse 129, CH-8600 Dübendorf, Switzerland
[2] Institute for Biomedical Engineering, Swiss Federal Institute for Technology (ETH) and University of Zürich, Moussonstrasse 18, CH-8044 Zürich, Switzerland
[3] Computer Vision Laboratory, Swiss Federal Institute for Technology, Gloriastrasse 32, CH-8044 Zürich, Switzerland

Received 6 May 2004
Published 6 August 2004
Online at stacks.iop.org/JPhysCM/16/S3499
doi:10.1088/0953-8984/16/33/011

Abstract

Advances in cell biology and tissue engineering rely heavily on performing 2D cell culture experiments. Analysis of these is conventionally done with 2D imaging techniques such as light (LM) or electron microscopy (SEM), since they are readily available. Cells, however, might act significantly differently when cultured in 2D or 3D environments. In order to analyse cells in a 3D arrangement, new imaging techniques are necessary not only in order to visualize the periphery of the cell culture in reflection mode but also to perform qualitative and quantitative investigations of the inner parts. Synchrotron radiation micro-computed tomography (SRμCT) using hard x-rays was shown to be a promising tool that can be used for 3D cell culture visualization. SRμCT allows not only visualization of cell cultures in their native 3D environment but also use of the volumetric nature of this imaging procedure to evaluate the cells quantitatively. In our approach, cells were seeded on polymer yarns, stained and measured with SRμCT in absorption and in differential absorption contrast mode. A new segmentation procedure was developed and the measured volumetric data were quantitatively assessed. Quantification parameters included total cell volume, total yarn volume, cell volume density, which is the ratio of cell to yarn volume, and the radial cell mass distribution. The applied variation of the staining parameter of gold enhancement incubation time was shown to have significant influence on the cell volume density. Differential absorption contrast mode was found to provide similar but no additional information on the investigated sample. Using novel approaches of hierarchical volumetric imaging allows closure of the gap between imaging of whole organs and single cells and might be expanded to even higher resolutions, offering investigation of the cell machinery in closer detail.

1. Introduction

Laboratory experiments in cell biology and tissue engineering are in general performed in flat 2D environments such as multi-well plates or cell culture dishes. This does not, however, resemble the natural states of living tissue, which is with a very few exceptions organized in a more or less complex 3D fashion. Moreover, it has been shown that cell behaviour in a 3D environment (Abbott and Cyranoski 2003) can deviate drastically from the behaviour in a 2D environment. This implies that experiments with cells in a 3D arrangement are necessary. Classical imaging techniques such as light microscopy (LM), scanning electron microscopy (SEM) or confocal laser scanning microscopy (CLSM) have only a limited feasibility for the investigation of such samples. Therefore, new imaging methods are needed. Previously we presented and validated synchrotron radiation micro-computed tomography (SRμCT) as a feasible tool for cell visualization (Thurner *et al* 2003). In contrast to CLSM for example, SRμCT is not limited to a maximum sample thickness and the use of transparent samples. Almost any combination of scaffolds with seeded cells can be investigated. With a limited spatial resolution of about 1 μm (Bonse and Busch 1996), SRμCT is a coarser technique as compared to CLSM or even more so to SEM. But due to the high brilliance of second and third generation synchrotron sources, and thus the use of monochromatic radiation, SRμCT delivers fully quantitative, isotropic 3D data. In contrast, LM and SEM imaging only allow visualization of external surfaces. Furthermore, in CLSM, being a comparable 3D imaging technique, the calibration of out-of plane dimensions is rather difficult due to aberration artifacts.

Tomography using x-rays is a well established technique that can be applied to very large (Marincek *et al* 2000) samples such as body parts and whole organs of humans down to the nanometre scale of a single cell (Weiß *et al* 2000). This means tomography can be used in a hierarchical fashion—from the human, to organ, tissue and down to the cell. Moreover, the volumetric nature of SRμCT measurements allows the quantitative assessment of cell cultures.

As shown previously (Thurner *et al* 2003), biological cells in a hydrated environment have to be stained using highly x-ray absorptive agents in order to produce sufficient contrast in acquired tomograms. In absorption contrast mode, which is most frequently used, a reconstructed tomogram consists essentially of a 3D mapping of the absorption coefficient α. For the extraction of quantitative information a segmentation procedure is needed in order to achieve a clear differentiation between stained cells and the surrounding scaffold and medium (the matrix). This is a non-trivial task since simple grey level based thresholding is not feasible here. In general, the histogram peaks of the matrix and the cells overlap in such samples, as can be seen in figure 1.

A procedure is introduced in the present communication, combining thresholding, component labelling and a morphological operator for effective cell segmentation. Since the amount of contrast agent deposited on the cells influences the contrast, we expect that the staining protocol has an influence on the quantitative information of the tomogram, especially on cell density and cell distribution. For this reason we defined an experiment where the staining protocol was varied, with respect to stain concentrations and incubation time. A total of six samples with different staining parameters were investigated.

Alternatively to the normal absorption contrast, differential absorption contrast (Bonse *et al* 1989) can be used to investigate stained cell cultures. The prerequisite for this technique is the presence of an absorption edge in the accessible energy range. In our experiments we used gold as a contrast agent, which offers its L I, L II, and L III edges at 14.4, 13.7, and 11.9 keV photon energy respectively. In theory, a sample that is measured above and below such an edge should yield a differential image representing the gold distribution within the

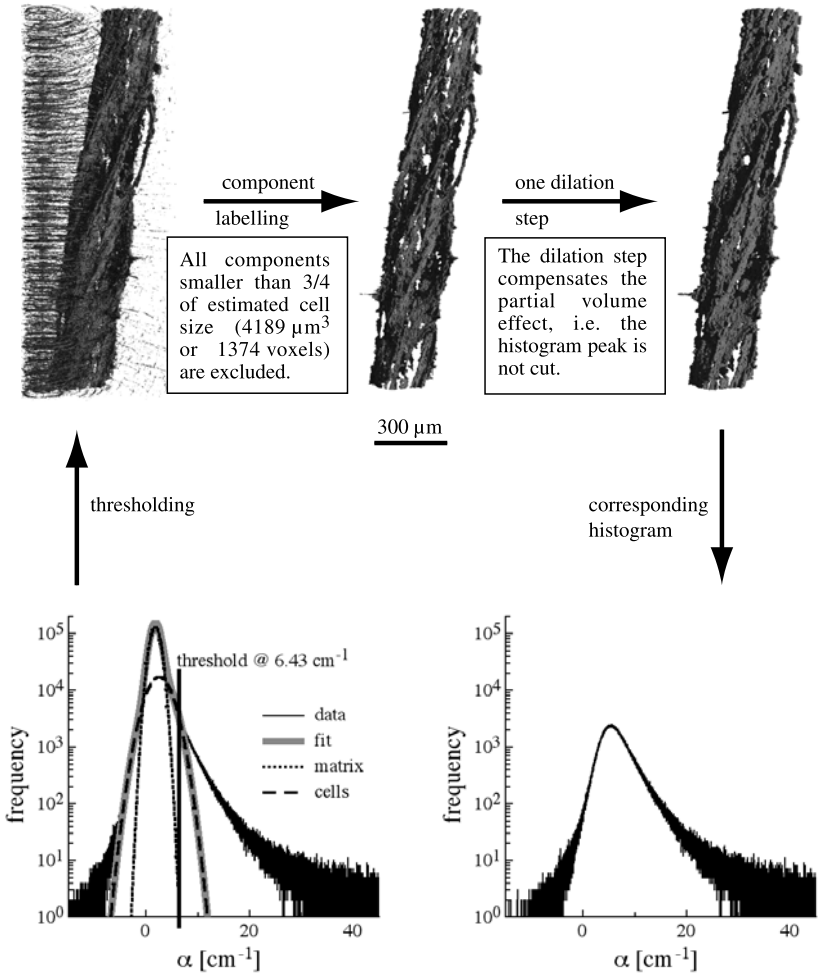

Figure 1. Scheme of cell segmentation. From the histogram of the cylindrical ROI, fitted with two Gaussians, the threshold is derived. The resulting data are 'cleaned', suppressing all components smaller than a single HFF cell, and dilated (enlarged) once to overcome the partial volume effect. The resulting histogram includes both sides of the cell peak. The sample is stained with 1:5 lectin in TBS for 3 h and gold enhanced for 5 min. Data are acquired at Beamline BW 2 at HASYLAB, photon energy 14.5 keV, spatial resolution 3.5 μm.

sample. It is therefore hypothesized further that the differential absorption contrast mode is feasible and beneficial for cell visualization.

2. Materials and methods

2.1. Sample preparation

The investigated cell cultures consisted of human foreskin fibroblasts (HFFs) seeded on polyethylene terephthalate (PET) multifilament yarns. The yarns are made of 32 filaments with a rounded polygonal shape and an outer diameter of about 20 μm. The exact pre-treatment of the yarns is described in detail elsewhere (Thurner *et al* 2003, p 399). The yarn pieces used for this

Table 1. Overview of variation of the staining protocol and quantified parameters for the different samples. Standard deviations are given in brackets where applicable.

Sample	1	2	3	4	5	6
Lectin concentration		1:5			1:10	
Lectin incubation time (h)		6			3	
Gold enhancement incubation time (min)	5	10	15	5	10	15
Total yarn volume (mm^3)	0.186	0.114	0.144	0.088	0.115	0.072
Total cell volume (mm^3)	0.023	0.025	0.033	0.013	0.026	0.027
CV/YV (%)	12.2	21.9	23.0	15.3	22.5	37.6
Cell density (mm^{-3})	29 000	52 000	55 000	37 000	54 000	89 000

study were all approximately 5 cm long. The cell number at seeding time was 10^5. The seeded yarns were put onto a 3D shaker installed in a cell incubator. After 3 days of incubation the samples were removed from the incubator and fixated in 2.5% glutaraldehyde in PBS for 5 h. Subsequently they were washed three times in PBS and stained. For SRμCT measurements the yarns were cut perpendicular to their long axes into two parts of equal length. One part was inserted in a thin walled glass vial filled with PBS. Then the vial was glued into a tomography sample holder and thus sealed.

2.2. Cell staining

All samples were stained using gold-labelled lectin (lectin from *Triticum vulgaris*, Sigma product number L1894) in tristate-buffered saline (TBS) and subsequently washed three times with PBS. The gold stain was amplified using a gold enhancement kit (Nanoprobes, Goldenhance—Lm/Blot). Prior to the gold enhancement all samples where washed twice in ultrapure water for 10 min. Then 200 μl of the gold enhancement solution were added for a given time. After this amplification process all samples were first washed with ultrapure water once, then twice with PBS, and finally they were stored in PBS at 4 °C until tomographic imaging. For one sample a combined gold-labelled lectin and osmium tetroxide (OsO_4) stain was applied. This sample was first stained with the lectin (concentration 1:10, incubation time 3 h) and the gold enhancement kit (incubation time 10 min) as mentioned above, and then incubated with post-fixative OsO_4 in PBS (concentration 2%, incubation time 2 h) and subsequently washed three times with PBS.

In order to test the effect of changes of the staining protocol on the acquired data six different samples were produced (see table 1). The samples were divided into two groups. Each group was either stained with the lectin using a higher concentration and a longer incubation time, i.e. 1:5 lectin in TBS applied for 6 h, or a lower concentration and a shorter incubation time, i.e. 1:10 lectin in TBS applied for 3 h. The gold enhancement in each group was increased stepwise, choosing incubation times of 5, 10, and 15 min.

2.3. SRμCT experiments

All tomography experiments were performed at Beamline BW2 at the Hamburger Synchrotronstrahlungslabor (HASYLAB) at the Deutsches Elektronen Synchrotron (DESY). For each sample 720 radiographic projections were recorded over a rotation angle of 180°, resulting in an angular step of 0.25° between two projections. The spatial resolution in a projection was determined to be 3.5 μm by calculating the modulation transfer function (MTF) from the radiographic projection of a gold edge (Müller *et al* 2002b). For the tomographic

reconstruction a filtered back-projection algorithm was used. The used photon energy of 14.5 keV for all samples scanned in absorption contrast mode was selected as it gave the highest contrast of the applied gold stain (Thurner *et al* 2003, Grodzins 1983). The sample prepared for differential absorption contrast was scanned at 14.5 keV above and at 11.8 keV below the gold L I, L II and L III edges. The rather large gap between the two photon energies was intentionally chosen. In order to detect the spatial distribution of osmium, a third measurement at even lower energy was performed. Consequently, only three tomograms are necessary instead of four, when the measurements are collected just above and below the absorption edges.

2.4. Data processing

In order to reduce the number of data a cylindrical region of interest (ROI) was selected for each sample containing only the cell-seeded yarn in PBS. The resulting histograms of all measurements (except the ones used for differential absorption contrast) were fitted with two Gaussians, one for the stained cells and one for the PBS and the yarn, using the Levenberg–Marquardt algorithm (ProFit, QuantumSoft, Uetikon am See, Switzerland). It should be noted here that the yarn itself does not contrast to the PBS.

2.5. Statistics

The significance of the influence of the staining protocol on quantified parameters was investigated using the analysis of variance (ANOVA) and the two-tailed Student t-test (StatView, Abacus Concepts, Berkeley, CA, USA). Both tests were done with a significance level p equal to 0.05.

3. Results

Previously we have shown that the intersection of the two Gaussians fitted to the histogram of absorption values, representing the matrix and the cells, can be used as a threshold to separate contrasted cell tissue from background (Müller *et al* 2002a). This threshold value is applicable for visualization using transparency-based rendering, but it is not very helpful for data binarization to the significant noise level. Therefore, the approach is modified as shown in figure 1. The threshold is shifted to the point where the Gaussian curve representing the matrix drops below the value of unity. By such a choice all voxels representing the matrix should vanish in the binarized tomogram. As demonstrated in figure 1, however, a limited number of voxels representing matrix are still visible. These few voxels are subsequently excluded using component labelling (Suzuki *et al* 2003). Here, particles in the dataset which are smaller than three-quarters of the average cell volume are removed. The cell volume of an HFF cell can be estimated to be equivalent to a sphere with a radius of 10 μm. Taking three-quarters of this value allows for a variation of the radius of about 10%, and can also be justified by the fact that the size of the cells is rather underestimated due to the thresholding. After component labelling the resulting volume is enlarged using a morphological dilation operation (Haralick *et al* 1987). It is applied once to overcome the partial volume effect and partly also the exclusion of voxels due to the thresholding. This procedure is certainly somewhat arbitrary. The retrieval of the original cell peak in the histogram indicates, however, the suitability of our approach.

Since all yarns are oriented parallel to the z-axis of the tomogram (perpendicular to the individual slices), the quantification of the binarized dataset is performed slice by slice as is depicted by the scheme in figure 2. From each slice containing now only stained cells the centre of mass is computed. From this the radial cell distribution, as well as a mean and

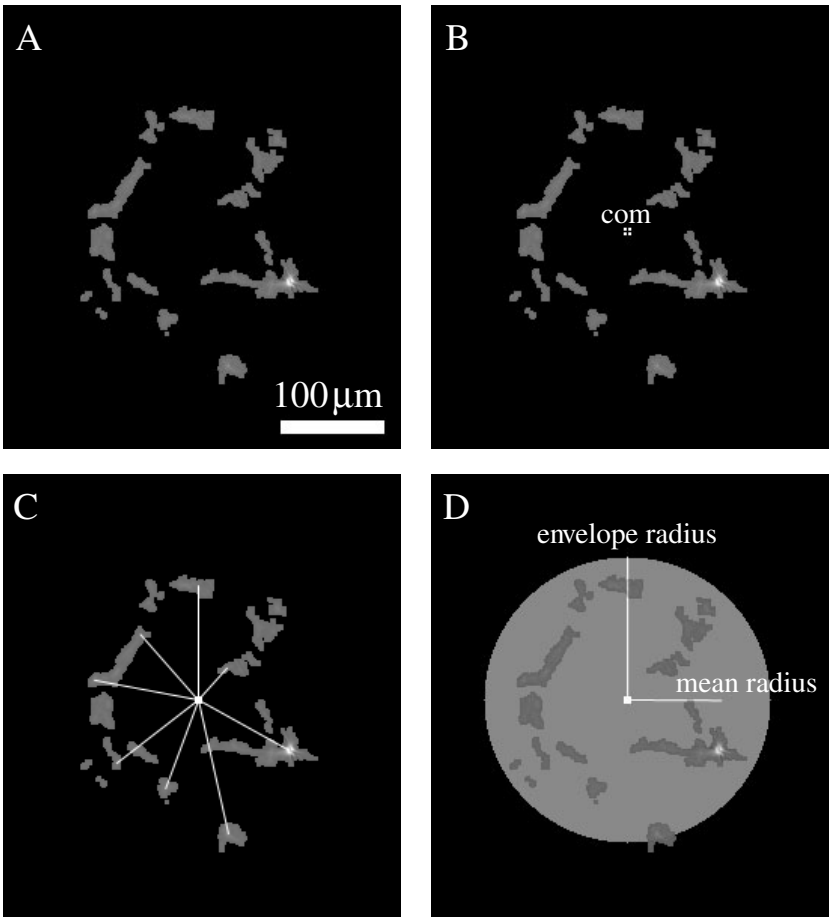

Figure 2. Sketch of the quantification procedure. All voxels in the single slice (A) representing stained cells (grey to white) are used to compute the centre of mass (COM) (B). From the COM the distances of all voxels are measured (C) and the mean and envelope (mean+2× standard deviations) radius (D) as well as the radial cell distribution are calculated.

an envelope radius, are derived. The envelope radius is defined as the mean radius plus two standard deviations containing now about 95% of the cells. The envelope radius is then used as a value for the volume of the bare yarn, of which *per se* no information can be retrieved. Summing over all slices the overall mean radius is calculated, as well as the total cell and the total yarn volume. From these values the ratio of cell volume to yarn volume (CV/YV) is derived, giving a normalized parameter of cell volume. Assuming an average cell volume of 4189 μm^3 as introduced already for component labelling, even an average cell density can be calculated. Results for the different parameters are summarized in table 1 for all six samples.

For the influence of the lectin concentration and lectin incubation time on the derived parameters the samples are divided in two groups of three samples: each with the same protocol for the lectin staining process. From figure 3 (top) it can be seen that the mean value of CV/YV is quite similar and the error bars representing the standard deviation overlap. Also the two-tailed Student t-test did not give evidence of significant difference ($p > 0.05$) between the two groups. Thus it seems the variation in the lectin stain protocol has no effect on the assessed parameters.

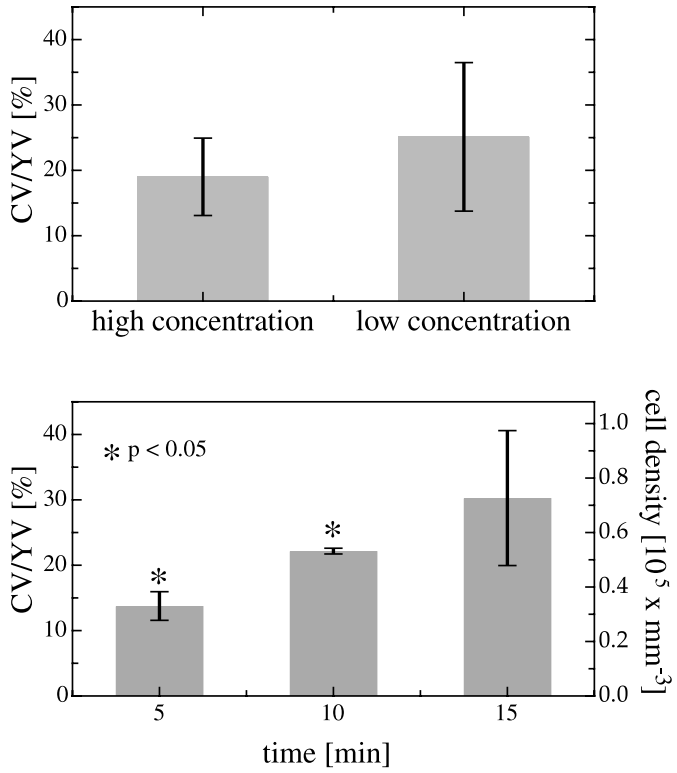

Figure 3. Cell volume/yarn volume (CV/YV) plotted versus concentration and incubation time of the lectin (top), and CV/YV plotted versus gold enhancement incubation time (bottom). Student's t-test gives a significant difference ($p < 0.05$) between groups with 5 and 10 min gold enhancement incubation time (bottom). The second y-axis (bottom) gives the estimated cell density. The group with 10 min incubation time is closest to the expected density of about 50 000 mm^{-3}.

Subsequently, the samples are regrouped in three groups of two samples each, where all samples in a group were exposed to the gold enhancement for the same time. The three mean values of the CV/YV and standard deviations are plotted versus the different groups in figure 3 (bottom). Clearly, a trend towards higher values with increasing incubation time of the gold enhancement is visible. Nevertheless, analysis of variance (ANOVA) for all three groups did not yield a statistically significant trend for the effect of incubation time. However, Student's t-test of CV/YV between the individual groups revealed that the 5 and 10 min groups differed significantly ($p < 0.05$). Overall, the trend seen in figure 3 (bottom) is expected and can be explained by the effect of the gold enhancement, which simply consists of gold ions that attach to already existing gold particles. The longer the stained yarn is exposed to the gold enhancement the more gold is deposited, which leads to higher cell numbers and thus higher CV/YV.

It was assumed that the gold enhancement is first effective on the yarn outside and at some later time, due to diffusion, on the yarn inside. If this is true then the relative number of cells inside the yarn should be higher for longer incubation time. The effect is investigated using the radial cell density plotted in figure 4. With increasing staining time the curve peak and area values rise. Yet, the ratio between cells on the 'outside' and cells on the 'inside', i.e. above and below the mean radius, only varies very slightly from 1.48 to 1.51 and 1.52 for 5, 10, and

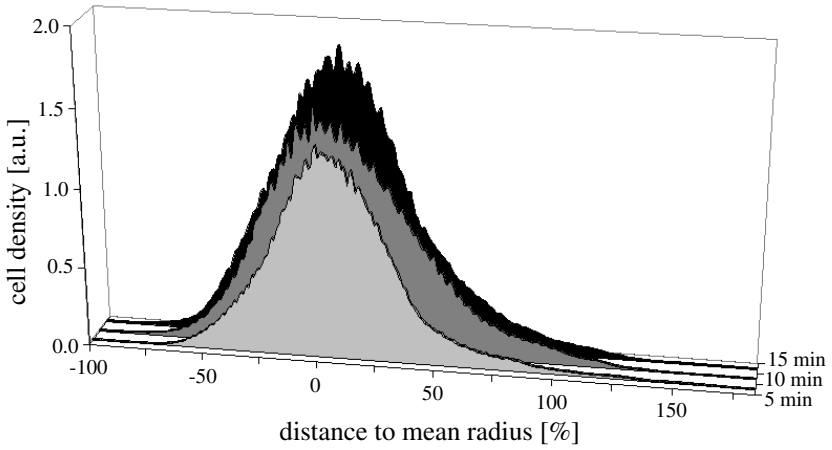

Figure 4. Average cell density plotted versus distance to the mean radius for all samples grouped according to gold enhancement incubation time. The main effect of increasing incubation time is the increase in cell density. The ratio between the area underneath the curve above and below the mean radius changes only very slightly from 1.48 to 1.52 but increases monotonically.

15 min gold enhancement incubation time, respectively, indicating that the stain penetrated the yarn even at the lowest exposure time.

In the case of differential absorption contrast mode the two datasets acquired below and above the gold L edges were subtracted from each other. Prior to that subtraction the datasets had to be matched using a rigid registration algorithm (Maes *et al* 1997). The reason for this was the fact that the yarn had moved slightly in between the two measurements and also during the first measurement. As a preprocessing step the initially chosen cylindrical ROI was reduced to stabilize the matching algorithm excluding artifacts in the first dataset arising from the slight sample movement. For the ROI reduction a high threshold, well above the intersection of the two fitted Gaussians in the histogram representing the matrix and the stained cells, was chosen. The choice was based upon exclusion of as many matrix voxels as possible. After thresholding the ROI was enlarged by several (up to ten) morphological dilation steps in order to retrieve the whole volume containing the stained cells and the yarn. After the registration the two matched datasets were subtracted from each other and masked with the ROIs of both precursor files. The histogram of the resulting dataset is shown in figure 5. Evidently, the differential absorption contrast did not give the output as expected; the stained cells did not simply show up as a well separated peak next to the matrix. On the contrary, again two overlapping peaks can be fitted into the final grey level distribution. The reason for this is clearly the too large separation of the two energies used and the resulting change in the absorption of the matrix. Thus the initial strategy, the performance of only three scans instead of four for differential absorption contrast of two different stains, was not profitable. The same segmentation and quantification procedure as used for absorption contrast was then applied to the differential absorption contrast dataset. The only difference was the first threshold, which was now set at the intersection of both curves in the histogram. A comparison of extracted quantitative parameters of the differential absorption contrast dataset and the one acquired at 14.5 keV is given in table 2. The values are in reasonable agreement with each other; differences are not larger than 10%. The remaining slight differences can be explained by the setting of ROIs in the case of differential absorption contrast mode. Due to this procedure some information

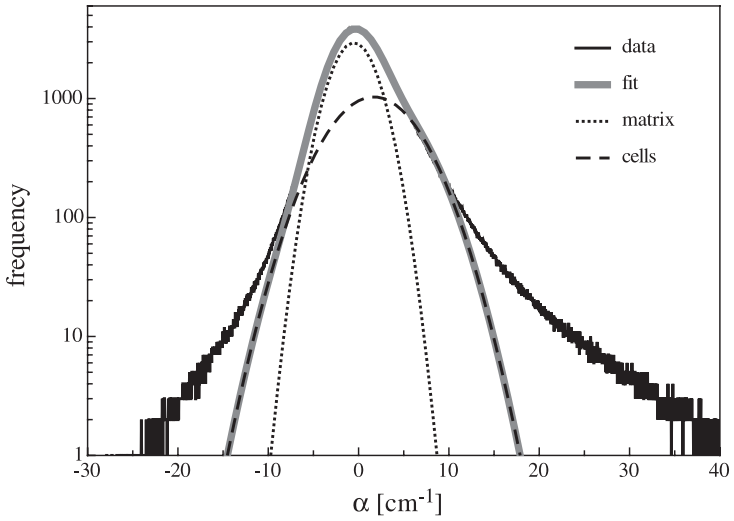

Figure 5. Resulting histogram retrieved of the two data sets used for differential absorption contrast. The histogram consisting of two overlapping peaks was fitted using two Gaussians representing the matrix and the stained cells respectively.

Table 2. Comparison of the results of the quantitative analysis applied to datasets acquired using absorption and differential absorption contrast mode.

Mode	Absorption contrast	Differential absorption contrast
Mean radius (μm)	93	92
Total yarn volume (mm^3)	0.111	0.100
Total cell volume (mm^3)	0.021	0.021
CV/YV (%)	19.1	20.8
Cell density (mm^{-3})	46 000	50 000

especially outside the yarn is lost. This is also supported by the 3D visualizations of both datasets given in figure 6. Clearly some parts of the stained cells still present in absorption contrast mode to the right-hand side (on the yarn outside) are missing in differential absorption contrast mode.

4. Discussion and conclusion

In this paper we have presented a novel procedure for segmentation and quantification of cell cultures imaged with SRμCT. Quantification parameters include total cell volume, total yarn volume, cell volume density, and the radial cell mass distribution. The applied variation of the gold enhancement incubation time was shown to have significant influence on the cell volume density. Differential absorption contrast mode was found to provide similar but not really additional information of the investigated sample.

The implemented image processing yields reasonable parameters, which is underlined by the histogram of the retrieved cell voxels shown in figure 1. In the segmentation procedure applied the threshold is actually set rather high in order to suppress most of the noise, prior to the component labelling. Doing so, some voxels of cellular structures are lost. This is especially

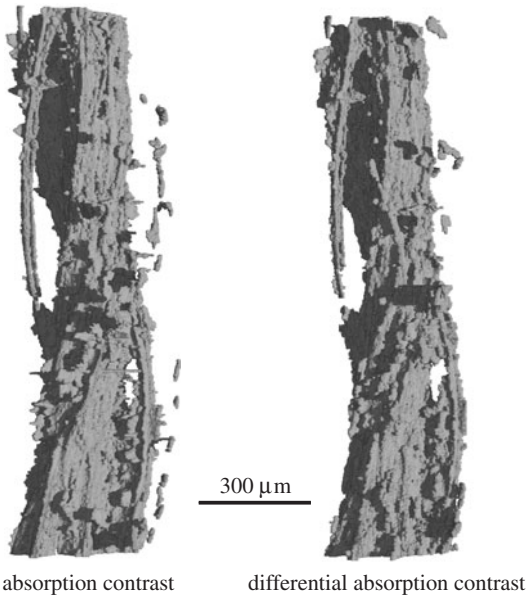

Figure 6. 3D visualization of the sample retrieved from absorption (scanned at 14.5 keV) and differential absorption contrast tomography (scanned at 11.8 and 14.5 keV). The two results are in good agreement with each other. Data acquired at Beamline BW 2 at HASYLAB, spatial resolution 3.5 μm.

important for the cell surface affected by the partial volume. In general, each component in the tomogram can be thought of being enveloped by a one-voxel-thick layer of partial volume. Since the morphological dilation operation enlarges a volume by expanding its surface voxel-wise, we assume that the single dilation operation step applied to each dataset regains the voxels lost due to the thresholding. This procedure may also assign a number of cavities. We believe, however, that this number of voxels is limited. The resulting error should be small, since the dilation operation is performed for all datasets in the same manner. Therefore, the procedure will only affect the results systemically (accuracy) and the group differences will be unaffected. Nevertheless, the values for CV, CV/TV, and cell density should be treated with care. It is necessary to confirm the quantified values using conventional cell counting techniques.

From the quantitative parameters resulting from the different staining procedures it can be concluded that the radial cell distribution is rather insensitive to the variation of the staining parameters. Further, there is no evidence of an influence of lectin concentration and incubation time on the outcome of the quantification. Thus a shorter staining duration using lower concentration seems feasible and should be recommended. The situation is different for the variation of the gold enhancement time. Although ANOVA testing did not reveal evidence that the variation of incubation time significantly explains the variation of the results for stained cell volume, Student's t-test of the 5 and 10 min gold enhancement groups showed a significant difference in CV/YV ($p < 0.05$). This behaviour is expected since the gold enhancement simply grows the initially deposited gold nanoparticles. The longer the exposure the bigger the particles will grow. In figure 3 (bottom) the secondary y-axis shows the estimated cell density (based on an assumed cell volume equal to a sphere with 10 μm radius). From the known cell number at seeding time it can be estimated that half of the cells will die during the

seeding process (due to the cell splitting process prior to this event). If a further half makes it to the yarn within 24 h and then doubles once or twice in the next 48 h, a cell density of about 50 000 cells mm^{-3} is retrieved. From the present results and our estimation of cell number, we recommend to stain cells on the yarn with a lectin concentration of 1:10 for 3 h and then incubate with the gold enhancement for 10 min. It should be noted, however, that this finding must be validated using a conventional cell counting technique, before a final conclusion can be made.

The differential absorption contrast did not prove to be beneficial to the segmentation of the stained cells. On the contrary, the situation became even more complicated since a matching algorithm had to be applied prior to the subtraction. The quantified parameters, however, proved to be reasonable compared to the ones acquired from the absorption contrast experiment. The situation might be drastically improved if the energies were chosen closer (e.g. 11.8 and 12.0 keV) together. Summarizing, it is noted that differential absorption contrast is not required if only one stain is applied. This changes when applying two or more different stains, sensitive to different cell features, i.e. cell membrane and cell nucleus. Then differential absorption contrast mode might deliver additional information, useful for quantification.

It should be noted that SRμCT is not competing against techniques such as CLSM but can yield complementary information; e.g. the presented model system is not fully accessible using CLSM due to the opaqueness of the scaffold. Furthermore, CLSM, although a 3D method, is prone to error of measured geometries in the z-direction. These errors even vary with depth, such that their correction is quite strenuous and requires the measurement of the point-spread function (PSF) in the z-direction at all depths (Gibson and Lanni 1991, McNally *et al* 1994). Even then the PSF is only true for an idealized system (the one used to determine it) and still systematic errors are encountered in geometry in the z-direction. Thus, despite the fact that CLSM is a readily available tool, the experimental and computational effort is quite high compared to SRμCT, where due to simple beam geometry and the monochromaticity the retrieved data are *per se* fully quantitative. Thus, although CLSM is of great value for cell imaging, SRμCT seems to be the method of choice if quantitative 3D information is needed and even more so if opaque scaffolds are used.

If we look into the future, we might want to explore the fact that in a 3D yarn system not only single experiments are possible. The yarn can be divided into multiple samples of one treatment state. Since the HFF cells have longest dimensions of about 50 μm (as investigated with LM) the yarn can be divided into individual sections with a 100 μm long gap in between. In our case, taking also a smallest sample length of 100 μm, a tomogram with 1024 voxels in the z-axis and 1.45 μm voxel length can be divided into seven independent measurements. This new 'multiple samples on a yarn' concept allows for better statistics, and fast measurements. The situation of quantified parameters will improve even more when performing such experiments at third generation SR sources. Due to edge enhancement also the light yarn filaments will give contrast at the yarn/cell and yarn/matrix interfaces. The inclusion of the scaffold geometry will allow conclusions about cell morphology and mechanical cell activity on the yarn. In summary, SRμCT proves to be a well suited tool for cell culture investigation and quantification in a non-destructive 3D fashion. Cells, seeded on polymer yarns, were stained and measured using SRμCT. A new segmentation procedure allowed the quantification of the volumetric data. Total cell volume, total yarn volume, cell volume density, and radial cell mass distribution were quantified. Gold enhancement incubation time was found to have a significant influence on cell volume density. Differential absorption contrast provides similar but no additional information compared to absorption contrast. Novel volumetric and hierarchical imaging approaches close the gap between imaging of whole organs and single cells and might be expanded to even higher resolutions, offering investigation of cell machinery in closer detail.

Acknowledgments

We are gratefully indebted to Felix Beckmann, for experimental SRμCT user support at the HASYLAB at DESY (II-99.077). We are equally grateful to Adrian Andronache for the performance of the rigid registration matching procedure and for giving advice in data pre-processing. Finally, we express our thanks to the Swiss National Science Foundation for financial support of this work (grant No 2153-057127.99).

References

Abbott A and Cyranoski D 2003 *Nature* **424** 870–2

Bonse U and Busch F 1996 *Prog. Biophys. Mol. Biol.* **65** 133–69

Bonse U, Nusshardt R, Busch F, Pahl R, Johnson Q C, Kinney J H, Saroyan R A and Nichols M C 1989 *Rev. Sci. Instrum.* **60** 2478–81

Gibson F S and Lanni F 1991 *J. Opt. Soc. Am.* A **8** 1601–13

Grodzins L 1983 *Nucl. Instrum. Methods* **206** 547–53

Haralick R M, Sternberg S R and Zhuang X 1987 *IEEE Trans. Pattern Anal. Mach. Intell.* **9** 523–50

Marincek B, Ros P R, Reiser M and Baker M E (ed) 2000 *Multislice CT—A Practical Guide* (Berlin: Springer) ISBN 3-540-41116-X

McNally J, Preza C, Conchello J A and Thomas L J Jr 1994 *J. Opt. Soc. Am.* A **11** 1056–67

Maes F, Collignon A, Vandermeulen D, Marchal G and Suetens P 1997 Multimodality image registration by maximization of mutual information *IEEE Transactions on Medical Imaging* **16** (2) 187–98

Müller B, Beckmann F, Huser M, Maspero F A, Szekely G, Ruffieux K, Thurner P and Wintermantel E 2002a *Biomol. Eng.* **19** 73–8

Müller B, Thurner P, Beckmann F, Weitkamp T, Rau C, Bernhardt R, Karamuk E, Eckert L, Buchloh S, Wintermantel E, Scharnweber D and Worch H 2002b *Proc. SPIE* **4503** 178–88

Suzuki K, Horiba I and Sugie N 2003 *Comput. Vis. Image Underst.* **89** 1–23

Thurner P, Müller B, Beckmann F, Weitkamp T, Rau C, Müller R, Hubbell J A and Sennhauser U 2003 *Nucl. Instrum. Methods* B **200** 397–405

Weiß D, Schneider G, Niemann B, Guttmann P, Rudoplh D and Schmahl G 2000 *Ultramicroscopy* **84** 185–97